

MOL #89268

Na⁺/H⁺ exchanger 1 is regulated via its lipid-interacting domain which functions as a molecular switch: A pharmacological approach using indolocarbazole compounds

Naoko Shimada-Shimizu, Takashi Hisamitsu, Tomoe Y. Nakamura, Noriaki Hirayama and Shigeo Wakabayashi

Department of Molecular Physiology, National Cerebral and Cardiovascular Center Research Institute (N.S.-S., T.H., T.Y.N., S.W.); and Basic Medical Science & Molecular Medicine, Tokai University School of Medicine (N.H.)

MOL #89268

Running title: Pharmacological evidence underlying the NHE1 regulation

Corresponding author: Shigeo Wakabayashi, Department of Molecular Physiology, National Cerebral and Cardiovascular Center Research Institute, Fujishirodai 5-7-1, Suita, Osaka 565-8565, Japan. Tel: 81-6-6833-5012 (ext. 2519); Fax: 06-6835-5314; E-mail: wak@ri.ncvc.go.jp

The number of text pages: 43

Tables: 0

Figures: 10

References: 32

The number of words in

Abstract: 223

Introduction: 728

Discussion: 1498

Abbreviations used: NHE1, Na⁺/H⁺ exchanger 1; pH_i, intracellular pH; LID, lipid-interacting domain; PKC, protein kinase C; MARCKS, myristoyl alanine-rich C-kinase substrate; DAG, diacylglycerol; PtdIns(4,5)P₂, phosphatidylinositol 4,5-bisphosphate; PE, phorbol ester; Phe, phenylephrine; PMA, phorbol-12-myristate-13-acetate; TNP-ATP, 2'3'-O-(2,4,6-trinitrophenyl)adenosine-5'-triphosphate tetra(triethylammonium); GFP, green fluorescent protein; HBS, Hepes-buffered saline; BCECF/AM, 2'7'-bis(2-carboxyethyl)-5(6)-carboxyfluorescein/acetoxymethyl.

MOL #89268

Abstract

The plasma membrane Na⁺/H⁺ exchanger 1 (NHE1) is rapidly activated in response to various stimuli. The membrane-proximal cytoplasmic region (~60 residues), termed the lipid-interacting domain (LID), is an important regulatory domain of NHE1. Here, we used a pharmacological approach to further characterize the role of LID in the regulation of NHE1. Pharmacological analysis using staurosporine-like indolocarbazole and bisindolylmaleimide compounds suggested that the phorbol ester- and receptor agonist-induced activation of NHE1 occurs through a protein kinase C-independent mechanism. In particular, only indolocarbazole compounds that inhibited NHE1 activation were able to interact with the LID, suggesting that the inhibition of NHE1 activation is achieved through the direct action of these compounds on the LID. Furthermore, in addition to phorbol esters and a receptor agonist, okadaic acid and hyperosmotic stress, which are known to activate NHE1 through unknown mechanisms, were also found to promote membrane association of the LID concomitant with NHE1 activation; these effects were inhibited by staurosporine as well as by a mutation in the LID. Binding experiments using the fluorescent ATP analog trinitrophenyl ATP revealed that ATP and the NHE1 activator phosphatidylinositol 4,5-bisphosphate bind competitively to the LID. These findings suggest that modulation of NHE1 activity by various activators and inhibitors occurs through the direct binding of these molecules to the LID, which alters the association of the LID with the plasma membrane.

MOL #89268

INTRODUCTION

The ubiquitous Na^+/H^+ exchanger isoform 1 (NHE1) catalyzes acid extrusion across the cell membrane by electroneutral ion exchange coupled to Na^+ influx, and serves as a key regulator of intracellular pH (pH_i), Na^+ concentration, and cell volume in virtually all tissues (Orlowski and Grinstein, 2004; Wakabayashi et al., 1997). NHE1 elicits relatively high exchange activity under unstimulated physiological conditions (basal state), and is further activated in response to various stimuli, including hormones, growth factors, and mechanical stress (activated state). This activation is attributable to a change in its affinity for intracellular H^+ ; thus, it can be easily detected in the neutral pH_i range as a stimuli-induced cytoplasmic alkalization in the absence of bicarbonate (Wakabayashi et al., 1997). While NHE1 activation plays a physiologically important role in optimizing the intracellular ionic environment, it is also thought to promote the pathogenesis of disease, such as heart failure and cancer (Cardone et al., 2005; Karmazyn et al., 2008; Wakabayashi et al., 2013). In fact, treatment with NHE1 inhibitors reduced the pathological phenotypes of animal models with acute and chronic heart diseases (Karmazyn et al., 2008).

The molecular mechanism of the hormonal activation of NHE1 has been the focus of many investigations. The stimulation of Gq-coupled receptors induces the hydrolysis of phosphatidylinositol 4,5-bisphosphate [$\text{PtdIns}(4,5)\text{P}_2$] via the activation of phospholipase C, which in turn produces 2 second messengers: diacylglycerol (DAG), which is a protein kinase

MOL #89268

C (PKC) activator, and inositol 1,4,5-triphosphate (IP₃), which leads to the release of calcium (Ca²⁺) from the endoplasmic reticulum through the IP₃ receptor (Taylor, 2002). Ca²⁺ was suggested to activate NHE1 via the direct interaction of Ca²⁺/calmodulin with the cytoplasmic domain of NHE1 during Ca²⁺-mobilization (Wakabayashi et al., 1994a). However, the role of DAG in NHE1 activation is controversial. The potent PKC activators, phorbol esters (PEs), activate NHE1; thus, PKC has long been believed to be a key molecule in the hormonal activation of NHE1 (Wakabayashi et al., 1997). However, NHE1 is not phosphorylated by PKC. We recently hypothesized that NHE1 is activated by the direct binding of DAG and PEs to the juxtamembrane cytoplasmic region of NHE1 and a subsequent conformational change of this region upon increased interaction with membrane lipids, rather than PKC (Wakabayashi et al., 2010). This region (aa 542–598) of NHE1 contains a cluster of cationic residues that interact with acidic phospholipids such as PtdIns(4,5)P₂ (Abu Jawdeh et al., 2011; Aharonovitz et al., 2000; Fuster et al., 2004) and hydrophobic residues, which are predicted to constitute a lipid-binding motif; therefore, we tentatively refer to it as the lipid-interacting domain (LID).

Many studies to date have used protein kinase inhibitors to determine whether NHE1 is regulated by phosphorylation. However, the reported effects of these inhibitors have led to ambiguous conclusions in many cases, i.e., different inhibitors targeting the same kinases produced variable effects. We predicted that some kinase inhibitors may inhibit NHE1

MOL #89268

regulation not via inhibition of PKC, but through a direct interaction with NHE1. Indeed, we previously reported that one such compound, staurosporine, abolished the PE- and receptor agonist-induced activation of NHE1, probably by interacting directly with the LID (Wakabayashi et al., 2010). Staurosporine belongs to a class of indolocarbazole compounds that are potential anticancer drugs (Sanchez et al., 2006). Various indolocarbazoles developed for pharmaceutical applications work by competing with ATP at ATP-binding sites of protein kinases (Nakano and Omura, 2009; Sanchez et al., 2006). The finding that staurosporine, which structurally resembles ATP, potently inhibits NHE1 regulation (Wakabayashi et al., 2010) led to our recent discovery that NHE1 is an ATP-binding protein and that ATP may directly activate NHE1 by interacting with the LID (Shimada-Shimizu et al., 2013). These findings raise the interesting possibility that the LID is a critical regulatory region that can interact with many activators and inhibitors. However, how NHE1 is regulated by these interactions remains unknown.

To address this question, we used a series of indolocarbazole and bisindolylmaleimide compounds that are potent protein kinase inhibitors. We first screened for drugs that inhibit PE- or receptor agonist-induced activation of NHE1, and found that—with the exception of a few compounds related to staurosporine—NHE1 regulation was not inhibited by most of the tested drugs. Furthermore, a few inhibitors competed with ATP for direct binding to the LID.

MOL #89268

These results suggest that the LID functions as a molecular switch that dictates the activation state of NHE1 in response to various stimuli.

MOL #89268

MATERIALS and METHODS

Chemical inhibitors and other reagents

Similarity-based virtual screening (Horio et al., 2007) of a chemical database containing approximately 5 million entities was performed using two reference structures (staurosporine and phorbol ester). Seventy of the top-ranking compounds were purchased from chemical suppliers through Namiki Shoji Co. Ltd. (Tokyo, Japan). Bisindolylmaleimide and indolocarbazole derivatives were purchased from Sigma-Aldrich Co. LLC (MO, USA), Merck Millipore (Darmstadt, Germany), and Toronto Research Chemicals Inc. (Ontario, Canada). Okadaic acid was purchased from Wako Pure Chemicals Ltd. (Osaka, Japan), and other phosphatase inhibitors were from CBC Co. Ltd. (NY, USA). These chemical compounds were dissolved in dimethylsulfoxide as 1 mM or 10 mM stock solutions and diluted into aqueous buffers immediately before use. The N-terminally biotinylated peptides corresponding to the cytoplasmic regions of NHE1 were synthesized with >85% purity by GL Biochem. Ltd. (Shanghai, China). GP57, GHHHWKDKLNRFNKKYVKKCLIAGERSKEPQLIAFYHKMEMKQAIELVESGGMGKIP ; LI-2A, GHHHWKDKLNRFNKKYVKKCLIAGERSKEPQAAAFYHKMEMKQAIELVESGGMGKI P; IL54, IRKILRNNLQKTRQLRSYNRHTLVADPYEEAWNQMLLRRQKARQLEQKINNYL. The

MOL #89268

amino acid sequences of GP57 and IL54 correspond to Gly-542–Pro-598 and Ile-631–Leu-684 of NHE1, respectively, while LI-2A corresponds to GP57 with Leu-573 and Ile-574 replaced by two Ala residues. [¹⁴C]benzoic acid, TNP-ATP and 1,2-dioctanoyl PtdIns(4,5)*P*₂ were obtained from PerkinElmer Life Science Inc. (MA, USA), Invitrogen (CA, USA), and Cayman Chem. Co. (MI, USA), respectively. All other reagents were of the highest purity available.

Molecular biology

The template plasmid carrying human NHE1 cDNA cloned into the pECE mammalian expression vector has been described previously (Wakabayashi et al., 2000). All constructs were generated via a PCR-based strategy as described previously (Wakabayashi et al., 2000). For construction of the GFP-tagged LID, the cytoplasmic region (aa 542–598) of NHE1 was amplified by PCR using pECE constructs as templates and inserted into the mammalian expression vector pEGFP-C1 (BD Biosciences Clontech, CA, USA) (Wakabayashi et al., 2010). For construction of myristoylated alanine-rich C-kinase substrate (MARCKS)-GFP, the entire coding region of cloned human MARCKS was inserted into the pEGFP-N1 vector (Wakabayashi et al., 2010). The mouse α 1-adrenergic receptor (α 1-AR) cDNA was purchased from Invitrogen and cloned into the expression vector pT-REx-DEST30 (Invitrogen). The DNA sequences of the PCR fragments were confirmed using a Model 3130 autosequencer (Applied Biosystems, MA, USA).

MOL #89268

Cells and transfection

The wild-type and mutant NHE1 constructs were transfected into exchanger-deficient PS120 cells (Pouyssegur et al., 1984) by Lipofectamine 2000 (Invitrogen), and stable NHE1 transfectants were prepared as described previously (Wakabayashi et al., 2000). NHE1 transfectants were further stably transfected with mouse α 1-AR under selection with G418.

Measurement of intracellular pH change

Extracellular stimuli-induced changes in pH_i were measured using the dual-excitation ratiometric pH indicator BCECF/AM, as previously described (Wakabayashi et al., 2010). Briefly, cells expressing the wild-type or mutant NHE1 variants were serum-depleted for more than 2 h and loaded with 0.3 μM BCECF/AM (Invitrogen) for 3 min at room temperature in HEPES-buffered saline (HBS) (140 mM NaCl, 2 mM CaCl_2 , 1 mM MgCl_2 , 5 mM glucose, and 20 mM HEPES/Tris, pH 7.0). Cells were then placed in a flow chamber connected to a perfusion system and superfused (0.6 ml/min) with HBS at 35°C. Fluorescence was measured at 510–530 nm with alternating excitations at 440 nm and 490 nm through a 505-nm dichroic reflector. Images were collected every 10–20 seconds using a cooled CCD camera (ORCA-ER, Hamamatsu photonics K.K., Japan) mounted on an inverted microscope (IX 71, Olympus) with a 20 \times objective (UApo/340, Olympus), and processed with AQUACOSMOS software

MOL #89268

(Hamamatsu Photonics). Changes in pH_i were monitored by switching perfusions from normal medium to HBS containing various reagents. The resting pH_i was calibrated as previously reported, using a high $[\text{K}^+]$ solution (containing 140 mM KCl, 2 mM CaCl_2 , 1 mM MgCl_2 , and 5 μM nigericin) and adjusted to various pH values ranging from 7.0 to 7.5. The change in pH_i was also measured by the ^{14}C benzoic acid-equilibration method (L'Allemain et al., 1984; Wakabayashi et al., 2010). In this experiment, serum-depleted cells were preincubated for 30 min in bicarbonate-free HEPES-buffered DMEM (pH 7.0), and then incubated in the same medium containing ^{14}C benzoic acid (1 $\mu\text{Ci}/\text{ml}$) and various agents for 15 min at 37°C. For the experiments measuring drug effect, cells were preincubated for 15 min in HEPES-buffered DMEM containing each inhibitor, and then switched to the radioisotope medium containing various stimuli and each inhibitor. After washing 4 times with ice-cold PBS, the cellular uptake of ^{14}C -radioactivity was measured. The change in pH_i was calculated according to the following equation: $\Delta\text{pH}_i = \log_{10} (^{14}\text{C}_{\text{stim}}/^{14}\text{C}_{\text{ref}})$, where $^{14}\text{C}_{\text{stim}}$ and $^{14}\text{C}_{\text{ref}}$ are the intracellular ^{14}C -radioactivity in the presence or absence of extracellular stimuli, respectively.

Confocal microscopy

Exchanger-deficient PS120 cells or PS120 cells stably expressing wild-type NHE1 were transfected with the GFP-labeled LID (aa 542–598) or GFP-labeled MARCKS for 6–8 h by Lipofectamine 2000 (Invitrogen). Cells were trypsinized and plated onto 35 mm glass-bottom

MOL #89268

dishes coated with collagen. Fluorescent signals were observed by confocal microscopy with an Olympus Fluoview FV1000 confocal microscope at 16–24 h after trypsinization. Various reagents were added directly to dishes at 22–25°C. Fluorescence intensities in the whole cells and in areas including plasma membrane were measured after selection by eye. For the MARCKS translocation analysis, fluorescence intensities in the plasma membrane (I_{mem}) and cytosol (I_{cyt}) were measured using Image-Pro Plus software (Media Cybernetics, Inc., MD, USA) and the ratio ($I_{\text{mem}}/I_{\text{cyt}}$) before and after addition of stimulant was calculated. The dissociation index was calculated as $(I_{\text{mem}}/I_{\text{cyt}})_{\text{before}}/(I_{\text{mem}}/I_{\text{cyt}})_{\text{after}}$.

Trinitrophenyl-ATP fluorescence measurement

TNP-ATP fluorescence was measured at room temperature in a buffer containing 100 mM NaCl, 1 mM MgCl₂ and 10 mM Hepes/Tris (pH 7.4) using a fluorometer (Hitachi F-7000) essentially as described previously (Guarnieri et al., 2011). Fluorescence data were obtained with emission and excitation wavelengths of 380 nm and 545 nm, respectively, using a quartz cuvette in a 500- μ L reaction volume. To examine the interaction between TNP-ATP and the peptide GP57, we carried out titration experiments, in which increasing concentrations of GP57 were added to a constant concentration of TNP-ATP (usually 20 μ M). To obtain the value of the dissociation constant (K_d) for TNP-ATP, we applied the following Langmuir single-site binding equation (Eq. 1) for a curve fit:

MOL #89268

$$\Delta F = (\Delta F_{\max}/2[T]_t) ((K_d + [P]_t + [T]_t) - \text{sqrt}((K_d + [P]_t + [T]_t)^2 - 4[P]_t[T]_t))$$

where ΔF is the observed fluorescence increase induced by the peptide, and $[P]_t$ and $[T]_t$ are total peptide and TNP-ATP concentrations, respectively. In the presence of competitors like staurosporine, we applied the following equation (Eq. 2) as described previously:

$$\Delta F = (\Delta F_{\max}/2[T]_t) ((K_d + (K_d/K_{d,C})[C]_t + [P]_t + [T]_t) - \text{sqrt}((K_d + (K_d/K_{d,C})[C]_t + [P]_t + [T]_t)^2 - 4[P]_t[T]_t))$$

where $K_{d,C}$ and $[C]_t$ are the dissociation constant and total concentration of competitor, respectively. Curve fitting was performed using GraphPad Prism (GraphPad Software, Inc., CA, USA) and the best-fitted values with standard error were obtained.

Statistical Analysis. Values are presented as the mean \pm S.D. values from three or more determinations. Data were analyzed with the Unpaired Student's *t* test for comparisons between two mean values. A value of $p < 0.05$ was considered significant.

MOL #89268

RESULTS

Phorbol ester- or hormone-induced activation of NHE1 is inhibited by only a few indolocarbazole compounds

We first screened for drugs that inhibit the stimulus-induced activation of NHE1. As shown in Fig. 1A, PMA induced a rapid cytoplasmic alkalinization of approximately 0.2 pH units in the NHE1 transfectants, as determined by pH_i monitoring with BCECF pH indicator dye. Such PMA-induced cytoplasmic alkalinization was also observed when pH_i was monitored by the ^{14}C -benzoic acid equilibration method (Fig. 2B). We used these methods to determine whether various chemical compounds inhibit NHE1 activation. For example, consistent with the previous report (Wakabayashi et al., 2010), staurosporine (St) almost completely abolished the PMA-induced activation of NHE1 (Fig. 1A and 2B). We challenged a screening of 70 chemicals (selected by virtual screening as described in the Materials and Methods). One such chemical N,2-diphenyl-4-propylimidazo[1,2a]benzimidazole-1-carbothioamide (designated drug 1) had no apparent inhibitory effect (Fig. 1A). Surprisingly, no significant inhibitory effects on PMA-induced cytoplasmic alkalinization were detected for any of the 70 chemicals. In addition, none of these compounds alone was able to induce cytoplasmic alkalinization. The chemical structures and effects on cytoplasmic alkalinization of the 18 top-ranking chemicals based on the similarity screening are shown in Supplemental Figs. S1 and S2, respectively.

MOL #89268

Given the results from screening of the initial 70 chemicals, we next focused on indolocarbazoles (e.g., staurosporine) and bisindolylmaleimides (BIS), which are all commercially available as inhibitors of PKC or other protein kinases (see Supplemental Figs. S3 and S4 for chemical structures). We first assessed the effect of these compounds on the basal exchange activity in the physiological neutral pH_i range. While staurosporine slightly reduced the resting pH_i at 1 μM , its higher concentration (10 μM) resulted in a clear cytoplasmic acidification (~ 0.2 pH unit) after a short lag phase, comparable to that observed for NHE1 inhibitor EIPA-induced acidification (Fig. 1B). However, staurosporine did not affect the surface expression level of NHE1 (Supplemental Fig. S5). These data are consistent with the previous finding that staurosporine inhibits the basal exchange activity by inducing the acidic shift of pH_i dependence, without change in the maximal exchange activity (V_{max}) (Wakabayashi et al., 2010). When the 30 compounds were assessed using the ^{14}C -benzoic acid equilibration method for 15 min at 1 μM , most of these chemicals alone had no effect on basal pH_i , although some drugs induced slight cytoplasmic acidification (Fig. 2A).

When the 30 compounds (at 1 μM) were used together with PMA, only a small number of compounds (9 out of 30) had an inhibitory effect on PMA-induced cytoplasmic alkalization (Fig. 2B). Of these, staurosporine, N-Bz-Staurosporine, UCN-01, and lestaurtinib were strongly inhibitory to PMA-induced cytoplasmic alkalization ($>80\%$ reduction), while BIS10, Go6976, UCN-02, K252a, and rebeccamycin exerted a mildly

MOL #89268

inhibitory effect (40–80% reduction) (see also Fig. 7 B–D and Supplemental Fig. S6 for concentration dependence of several other drugs). The inhibitory effect of K252a is consistent with the experiment using BCECF, in which K252a was also shown to be inhibitory (see Fig. 1B).

Next, we examined the effects of these 30 compounds on the activation of NHE1 in response to Gq-coupled receptor agonist. The NHE1 transfectants were further stably transfected with the α 1-adrenergic receptor (α 1-AR) and the cells were stimulated with the receptor agonist phenylephrine (Phe). Stimulation with Phe resulted in a large cytoplasmic alkalinization only in the NHE1 transfectants expressing α 1-AR (Fig. 3). Similar to the results for PMA-induced alkalinization, none of the compounds, other than staurosporine, had a strong inhibitory effect on Phe-induced cytoplasmic alkalinization at 1 μ M (Fig. 3). Notably, N-Bz-staurosporine, UCN-01, K252a, and lestaurtinib exerted only a marginal inhibition of Phe-induced cytoplasmic alkalinization at 1 μ M (Fig. 3), although they were more effective when PMA was used (Fig. 2B). However, we observed that each of these 4 compounds resulted in almost complete inhibition of phenylephrine-induced cytoplasmic alkalinization when used at 10 μ M (data not shown, but see Supplemental Fig. S7 for concentration dependence of several drugs). The results of this screen indicated that the majority of protein kinase inhibitors, with a few exceptions, had no effect on PE- or hormone-induced activation of NHE1.

MOL #89268

Most indolocarbazole compounds inhibit PKC in cells

To determine whether the 30 indolocarbazole and BIS compounds could inhibit PKC at the concentration used for pH_i measurement (1 μ M), we evaluated the effects of the compounds by using fluorescently tagged MARCKS, which is a PKC substrate known to dissociate from the plasma membrane in response to PKC-mediated phosphorylation (Ohmori et al., 2000). In fact, PMA resulted in a nearly complete dissociation of MARCKS-GFP from the plasma membrane after 15 min incubation (Fig. 4A, leftmost panels). Staurosporine, UCN-01, and K252a, which inhibited the PMA-induced activation of NHE1, abrogated the PMA-induced MARCKS-GFP translocation at 1 μ M (Fig. 4A). However, BIS1, BIS2, KT5823, and K252b, which did not affect the PMA-induced activation of NHE1, also almost completely abolished the PMA-induced MARCKS-GFP translocation at 1 μ M (Fig. 4A). These data indicate that these compounds can inhibit PKC under the similar conditions used for pH_i measurement, regardless of their effects on NHE1 activation. Among the 30 compounds tested, all except for drug 1 and SB218078 significantly inhibited MARCKS-GFP translocation, as shown by a decrease in the dissociation index (Fig. 4B), indicating that these 28 drugs were indeed capable of inhibiting PKC at 1 μ M. Taken together, these data suggest that PMA- or receptor agonist-induced activation of NHE1 occurs through a PKC-independent mechanism.

MOL #89268

Indolocarbazole compounds that block NHE1 activation interact with a peptide corresponding to the LID of NHE1

As described above, only a few drugs were shown to block the PMA- or agonist-induced activation of NHE1 (Figs. 2B and 3). We predicted that effective compounds such as staurosporine interact directly with the LID, which is the critical regulatory domain of NHE1.

Attempts to determine whether staurosporine interacts with the LID were hampered by the non-specific interaction of this drug with the affinity beads and dialysis bags used to study protein-ligand interaction, and also by interference from the strong fluorescence of staurosporine. We assessed the interaction of various compounds with an LID-derived peptide (GP57) by using the fluorescent ATP analog trinitrophenyl ATP (TNP-ATP) (Guarnieri et al., 2011). Based on our previous finding that ATP binds to the LID (Shimada-Shimizu et al., 2013), it was expected that any molecule that can interact with the LID would compete with ATP for binding.

We first determined whether TNP-ATP is a suitable reporter for monitoring the interaction of compounds with the LID. The intensity of TNP-ATP fluorescence increased upon incubation with GP57, with a slight blue shift in the emission spectrum (Fig. 5A), indicating the interaction of TNP-ATP with GP57. TNP-ATP fluorescence reached saturation at higher GP57 concentrations (Fig. 5B); the dissociation constant (K_d) for TNP-ATP was determined to be $28.0 \pm 1.8 \mu\text{M}$. The presence of non-fluorescent ATP (5 mM) reduced the

MOL #89268

affinity of TNP-ATP for GP57, i.e., the titration curve did not show saturation at concentrations less than 150 μM of GP57 (Fig. 5B); the K_d for ATP binding to GP57 was $430 \pm 43 \mu\text{M}$. Similarly, the inclusion of water-soluble $\text{PtdIns}(4,5)P_2$, a putative activator of NHE1, reduced the affinity of TNP-ATP for GP57 (Fig. 5B), with a K_d of $22.3 \pm 6.9 \mu\text{M}$ for $\text{PtdIns}(4,5)P_2$ binding to GP57. These data suggest that $\text{PtdIns}(4,5)P_2$ and ATP compete with TNP-ATP for binding to the LID. The increase in TNP-ATP fluorescence was not observed upon incubation with a control peptide, IL54 (Fig. 5A). The mutation of two hydrophobic residues of the LID (Leu-573 and Ile-574) to alanine in the LI-2A peptide also abolished the peptide-induced increase in TNP-ATP fluorescence (Fig. 5A), suggesting that these residues are critical for the binding of ATP to the LID.

A similar displacement assay was used to assess the interaction of chemical compounds with GP57. While staurosporine itself emitted fluorescence (Fig. 6A, upper middle trace), it greatly reduced the GP57-induced fluorescence increase of TNP-ATP (Fig. 6A, compare upper left and upper middle traces), suggesting that staurosporine inhibits the interaction of TNP-ATP with GP57. Similarly, in the presence of UCN-01 or K252a, the GP57-induced fluorescence increase was reduced compared to the control (Fig. 6A). In contrast, BIS1 and arcyriaflavin A did not notably affect the TNP-ATP fluorescence (Fig. 6A). The effects of all 30 compounds on the GP57-induced increase in TNP-ATP fluorescence are shown in Fig. 6B. Interestingly, several of the compounds that inhibited NHE1 activation at a low concentration

MOL #89268

(staurosporine, N-Bz-staurosporine, UCN-01, UCN-02, and K252a; see Fig. 2B) reduced the GP57-induced increase in TNP-ATP fluorescence (Fig. 6B). Conversely, the compounds that did not affect NHE1 activation did not affect TNP-ATP fluorescence (Fig. 6B). This apparent correlation between drug-induced inhibitions of NHE1 activation and TNP-ATP fluorescence is consistent with the notion that the inhibition of NHE1 activation occurs through a direct interaction of indolocarbazole compounds with the LID. Analysis of the dose-dependence of GP57 in the presence of competitive drugs indicated that staurosporine, UCN-01, and K252a interact with GP57 with K_d values of $1.70 \pm 0.05 \mu\text{M}$, $2.54 \pm 0.13 \mu\text{M}$, and $3.35 \pm 0.08 \mu\text{M}$, respectively (Fig. 7A). These drugs inhibited the PMA-induced activation of NHE1 within a similar range of concentrations (Fig. 7B–D). These results provide evidence that these effective compounds inhibit the PMA- or agonist-induced activation of NHE1 through a direct interaction with the LID, and not by inhibiting protein kinase activity.

Staurosporine can inhibit NHE1 activation induced by okadaic acid and hyperosmotic stress

We next examined whether staurosporine could inhibit NHE1 activation induced by stimuli that are not known to activate PKC. We found that the phosphatase inhibitor okadaic acid, which was previously reported to activate NHE1 (Sardet et al., 1991), indeed induced a large cytoplasmic alkalinization (Fig. 8A). This activation was completely blocked by $1 \mu\text{M}$ of

MOL #89268

staurosporine (Fig. 8A). At higher concentrations (>10 μ M), staurosporine also inhibited NHE1 activation induced by hyperosmotic stress, which is also reported to activate NHE1 with unknown mechanism (Fig. 8B). Okadaic acid and hyperosmotic stress did not promote MARKCS-GFP dissociation from the plasma membrane in the presence or absence of staurosporine (Fig. 8C, D), while PMA did so even in the presence of okadaic acid (Fig. 8C, right panels). These results indicate that PKC-independent mechanisms underlie the NHE1 activation induced by okadaic acid and hyperosmotic stress as well as the staurosporine-mediated inhibition of NHE1 activation. Furthermore, in contrast to okadaic acid, all other phosphatase inhibitors did not affect pH_i (Fig. 8A); thus, NHE1 activation by okadaic acid occurs through a mechanism, which is not due to the inhibition of protein phosphatase activity. Importantly, the mutation of hydrophobic residues in the LID (LI-2A) abolished or greatly reduced the NHE1 activation induced by okadaic acid and hyperosmotic stress (also observed for PMA and α 1-AR agonist) (Fig. 8E), suggesting that the NHE1 activation induced by these stimuli also occurs through the LID.

Staurosporine inhibits the plasma membrane translocation of the GFP-labeled LID induced by various stimuli

We previously suggested that NHE1 activation occurs via a direct interaction of PEs/DAG and a subsequent conformational change of the LID accompanied by increased affinity with

MOL #89268

membrane lipids (Wakabayashi et al., 2010). To assess the effects of staurosporine on this process, we monitored changes in the membrane association using a GFP-labeled LID probe as described previously (Wakabayashi et al., 2010). Under unstimulated conditions, GFP-LID was mainly localized within the nucleus because of the nuclear localization tendency of GFP itself (Fig. 9A and B). PMA promoted the plasma membrane translocation of GFP-LID (Fig. 9B), suggesting that PMA increases the affinity of the LID for the membrane lipids. This translocation was inhibited by staurosporine, which can interact with the LID, but not by BIS1 (Fig. 9B). Interestingly, Phe (Fig. 9C), okadaic acid (Fig. 9D), and hyperosmotic stress (Fig. 9E) also promoted the plasma membrane translocation of the LID, which was inhibited by staurosporine in all cases. These results suggest that the extent of membrane association of LID determines the NHE1 activation induced by various stimuli.

The depletion of cellular ATP is known to drastically inhibit the exchange activity of NHE1 and render it inactive in response to various stimuli (Cassel et al., 1986; Little et al., 1988; Wakabayashi et al., 1997) (see Fig. 8E). We found that ATP depletion abrogated the PMA-induced plasma membrane translocation of the LID (Fig. 9F), while PMA was able to promote the nuclear export of the LID. Furthermore, in PMA-stimulated cells, incubation for 15 min in 5 mM 2-deoxyglucose, which was reported to deplete ATP to less than 2% (Shimada-Shimizu et al., 2013), gradually removed the LID from the plasma membrane (Fig.

MOL #89268

9G). These data suggest that the continuous existence of ATP is required for the association of the LID with the plasma membrane.

MOL #89268

DISCUSSION

In this study, we addressed the role of the LID in regulation of NHE1 mainly by pharmacological approach as an extension of our previous work (Wakabayashi et al., 2010). Our new findings obtained in this work are summarized as follows: (1) Among diverse array of staurosporine derivatives or other tested compounds, only a few chemicals directly binds to the LID in competition with ATP at low concentration and effectively inhibits NHE1 activation in response to PEs and receptor agonist, providing evidence that inhibition of NHE1 regulation by these chemicals is mediated via direct action on the LID, rather than inhibition of protein kinases. (2) In addition to phorbol esters and receptor agonist, okadaic acid and hyperosmotic stress promoted the translocation of a GFP-tagged LID to the plasma membrane concomitant with NHE1 activation, and these effects were inhibited by staurosporine as well as the LID mutation. Thus, the LID functions as a key element to receive diverse signals and plasma membrane association of LID determine the activity-state of NHE1. (3) ATP depletion blocks the LID interaction to the plasma membrane concomitant with the drastic inhibition of NHE1 activity, and ATP and $\text{PtdIns}(4,5)\text{P}_2$ alternatively interact with the LID, suggesting that the basal exchange activity is preserved by the interaction of ATP and/or acidic membrane lipids to the LID.

Most indolocarbazole or bisindolylmaleimide compounds are known to inhibit protein kinases such as PKC at submicromolar concentrations. Importantly, many of these chemicals

MOL #89268

did not inhibit NHE1 activation induced by phorbol esters or receptor agonists at 1 μ M (Figs. 2 and 3), while they did inhibit PKC under similar conditions, as shown by the inhibition of MARCKS-GFP removal from the plasma membrane (Fig. 4). One could argue that these compounds may be inert for certain PKC isozymes that are not involved in MARCKS phosphorylation. However, at least some of these drugs can inhibit various PKC isozymes at submicromolar concentrations. For example, BIS1 potently inhibits the PKC α , β _I, β _{II}, γ , δ , and ϵ -isozymes (Heikkila et al., 1993; Toullec et al., 1991), but did not inhibit NHE1 activation in our study. These data strongly suggest that a large part of NHE1 activation occurs through a PKC-independent mechanism. Furthermore, except for okadaic acid, no other potent phosphatase inhibitor induced cytoplasmic alkalinization (Fig. 8A). The inert properties of many protein kinase/phosphatase inhibitors argue against the concept that NHE1 is regulated via a phosphorylation-dephosphorylation balance.

The inhibition of NHE1 activation appears to occur via direct interactions of a few effective drugs with LID. Consistent with the previous ²²Na⁺ uptake data (Wakabayashi et al., 2010), staurosporine reduced the resting pH_i (Fig. 1B), suggesting that staurosporine inhibits the basal exchange activity by directly interacting with NHE1, probably via the LID. Notably, the effective dose of the inhibitors varied with the different stimuli: for example, N-Bz-staurosporine, UCN-01, and lestaurtinib inhibited PMA-induced activation at 1 μ M, but

MOL #89268

not receptor agonist-induced activation. Such a difference may be due to the activating substances that interact with the LID (PMA vs. DAG).

In the present study, we found that PtdIns(4,5) P_2 reduces the binding affinity of TNP-ATP with the GP57 LID-derived peptide (Fig. 5B). Additionally, PtdIns(4,5) P_2 inhibited the equilibrium binding of [$\gamma^{33}\text{P}$]ATP to GP57 (data not shown). These findings suggest that ATP can be at least partly replaced by PtdIns(4,5) P_2 as a binding partner of the LID. Acidic lipids such as PtdIns(4,5) P_2 and phosphatidylserine are known to interact with the cationic regions of the LID of NHE1, and the mutation of cationic or hydrophobic residues in the LID abrogated the interaction of the LID with acidic lipids and reduced the basal exchange activity (Aharonovitz et al., 2000; Wakabayashi et al., 2010). Furthermore, the present study indicated that one such mutation (LI-2A) blocked the interaction of the LID with TNP-ATP (Fig. 5A). These findings, together with previous data (Shimada-Shimizu et al., 2013), suggest that in addition to acidic phospholipids, ATP also plays an important role in maintaining the basal activity of NHE1. Indeed, a study using whole-cell patch clamp technique has revealed that NHE1 activity, which had been once abolished by ATP depletion was able to be restored by perfusion with PtdIns(4,5) P_2 inside the cells (Fuster et al., 2004). However, GFP-LID was primarily localized in the plasma membrane upon stimulation, but not in the resting state (Fig. 9). These findings raise the possibility that ATP, rather than acidic phospholipids, may be a major cofactor for preserving the basal exchange activity, and the exchange from ATP to

MOL #89268

acidic phospholipids occurs upon activation of NHE1 in response to stimulants, presumably via a conformational change of the LID.

Based on the current and previous data (Wakabayashi et al., 2010), we present a model for NHE1 regulation via the LID (Fig. 10). PEs/DAG directly interact with the LID and induce the translocation of the LID to the plasma membrane, resulting in NHE1 activation. Staurosporine derivatives or LID mutations abolish these processes, and thus inhibit NHE1 regulation. According to this model, movement of the juxtamembrane region of NHE1 (i.e., the LID) toward or away from the lipid bilayer determines the activation state of NHE1, possibly by modulating H⁺ affinity. From the negative results obtained using various protein kinase inhibitors, we propose that NHE1 phosphorylation makes a negligible contribution to PE- or agonist-induced NHE1 activation, consistent with the conclusions of our previous study (Wakabayashi et al., 1994b). In the resting state, ATP or acidic phospholipids would bind to the LID and maintain the basal exchange activity (Fig. 10). In contrast, ATP depletion would primarily promote dissociation of ATP from NHE1 and simultaneously reduce the level of PtdIns(4,5)P₂ by facilitating its dephosphorylation. In fact, we observed that ATP depletion promoted the removal of the LID from the plasma membrane (Fig. 9F and G). Thus, ATP depletion drastically inhibits basal exchange activity and renders NHE1 unresponsive for various stimuli. Indolocarbazoles directly interact with the LID and inhibit the interaction of ATP or acidic phospholipids with LID. Several pieces of evidence in this study suggest that

MOL #89268

NHE1 activation in response to okadaic acid and hyperosmolarity may also occur via the LID:

(i) staurosporine inhibited the activation of NHE1 induced by these stimuli (Fig. 8); (ii) these stimuli facilitated the plasma membrane translocation of the LID, which was inhibited by staurosporine (Fig. 9C and D); and (iii) mutation of hydrophobic residues (LI-2A) in the LID abolished NHE1 activation in response to these stimuli (Fig. 8E). Thus, we propose that the LID is the key regulatory domain of NHE1, and receives diverse signals that affect the modulation of exchange activity (i.e., the LID functions as a molecular switch). Thus, the pH_i -dependence of exchange activity is controlled by species and effective doses of substances that interact with NHE1 through its LID.

The variable effects of protein kinase inhibitors that have been previously reported, in many cases, led to ambiguous conclusions, likely because the possibility of a direct action of these inhibitors on NHE1 was not considered. Our present results suggest the structural preference of a few chemicals for the LID of NHE1. The effectiveness of the compounds on NHE1 is clearly different from that on protein kinases. Staurosporine derivatives are indolocarbazole alkaloids containing similar structures, including an indole[2,3- α]carbazole core with a C-N linkage to a sugar moiety (Supplemental Figs. S3 and S4). Since bisindolylmaleimide derivatives did not affect NHE1 at least at low concentration, the presence of at least the γ -lactam ring and sugar moiety (Supplemental Fig. S4) appears to be important for inhibition of NHE1 activation. The lactam ring and sugar moieties of

MOL #89268

staurosporine are analogous to the adenine ring and ribose moieties of ATP, respectively (Toledo and Lydon, 1997). In fact, these moieties were shown to be important for the interaction of staurosporine with ATP-binding sites in the crystal structures of staurosporine-bound phosphoinositide 3-kinase (Walker et al., 2000), cAMP-dependent kinase, and cyclin-dependent kinase 2 (Toledo and Lydon, 1997). Our present study provides an important step for elucidating the structural basis of NHE1 regulation.

The activation of NHE1 is linked to various diseases such as heart failure and cancer. We previously reported that the activation of NHE1 is sufficient to induce cardiac hypertrophy and heart failure (Nakamura et al., 2008). While NHE1 inhibitors such as cariporide, which completely shuts off the ion transport were shown to prevent ischemia-reperfusion injury and chronic heart failure in animal models (Baartscheer et al., 2008; Huber et al., 2012; Karmazyn et al., 2008), they did not clearly show the beneficial effects on patients in several clinical trials (Karmazyn, 2013). A specific drug that selectively inhibits only the regulation of NHE1 while preserving its transport activity may be useful as a new therapeutic approach against heart failure.

MOL #89268

Author Contributions

Participated in research design: Shimada-Shimizu, N., and Wakabayashi, S.

Conducted experiments: Shimada-Shimizu, N., Hisamitsu, T., and Wakabayashi, S.

Contributed drug selection: Hirayama, N.

Performed data analysis: Shimada-Shimizu, N., and Wakabayashi, S.

Wrote or contributed to the writing of the manuscript: Nakamura, Y.T., and Wakabayashi, S.

MOL #89268

REFERENCES

- Abu Jawdeh, BG, Khan, S, Deschenes, I, Hoshi, M, Goel, M, Lock, JT, Shinlapawittayatorn, K, Babcock, G, Lakhe-Reddy, S, DeCaro, G, et al. (2011). Phosphoinositide binding differentially regulates NHE1 Na^+/H^+ exchanger-dependent proximal tubule cell survival. *J Biol Chem* 286, 42435-42445.
- Aharonovitz, O, Zaun, HC, Balla, T, York, JD, Orłowski, J, and Grinstein, S (2000). Intracellular pH regulation by Na^+/H^+ exchange requires phosphatidylinositol 4,5-bisphosphate. *J Cell Biol* 150, 213-224.
- Baartscheer, A, Hardziyenka, M, Schumacher, CA, Belterman, CN, van Borren, MM, Verkerk, AO, Coronel, R, and Fiolet, JW (2008). Chronic inhibition of the Na^+/H^+ - exchanger causes regression of hypertrophy, heart failure, and ionic and electrophysiological remodelling. *Br J Pharmacol* 154, 1266-1275.
- Cardone, RA, Casavola, V, and Reshkin, SJ (2005). The role of disturbed pH dynamics and the Na^+/H^+ exchanger in metastasis. *Nat Rev Cancer* 5, 786-795.
- Cassel, D, Katz, M, and Rotman, M (1986). Depletion of cellular ATP inhibits Na^+/H^+ antiport in cultured human cells. Modulation of the regulatory effect of intracellular protons on the antiporter activity. *J Biol Chem* 261, 5460-5466.
- Fuster, D, Moe, OW, and Hilgemann, DW (2004). Lipid- and mechanosensitivities of sodium/hydrogen exchangers analyzed by electrical methods. *Proc Natl Acad Sci U S A*

MOL #89268

101, 10482-10487.

Guarnieri, MT, Blagg, BS, and Zhao, R (2011). A high-throughput TNP-ATP displacement assay for screening inhibitors of ATP-binding in bacterial histidine kinases. *Assay Drug Dev Technol* 9, 174-183.

Heikkila, J, Jalava, A, and Eriksson, K (1993). The selective protein kinase C inhibitor GF 109203X inhibits phorbol ester-induced morphological and functional differentiation of SH-SY5Y human neuroblastoma cells. *Biochem Biophys Res Commun* 197, 1185-1193.

Horio, K, Muta, H, Goto, J, and Hirayama, N (2007). A simple method to improve the odds in finding 'lead-like' compounds from chemical libraries. *Chem Pharm Bull (Tokyo)* 55, 980-984.

Huber, JD, Bentzien, J, Boyer, SJ, Burke, J, De Lombaert, S, Eickmeier, C, Guo, X, Haist, JV, Hickey, ER, Kaplita, P, et al. (2012). Identification of a potent sodium hydrogen exchanger isoform 1 (NHE1) inhibitor with a suitable profile for chronic dosing and demonstrated cardioprotective effects in a preclinical model of myocardial infarction in the rat. *J Med Chem* 55, 7114-7140.

Karmazyn, M (2013). NHE-1: Still a viable therapeutic target. *J Mol Cell Cardiol*.

Karmazyn, M, Kilic, A, and Javadov, S (2008). The role of NHE-1 in myocardial hypertrophy and remodelling. *J Mol Cell Cardiol* 44, 647-653.

L'Allemain, G, Paris, S, and Pouyssegur, J (1984). Growth factor action and intracellular pH

MOL #89268

regulation in fibroblasts. Evidence for a major role of the Na^+/H^+ antiport. *J Biol Chem* 259, 5809-5815.

Little, PJ, Weissberg, PL, Cragoe, EJ, Jr., and Bobik, A (1988). Dependence of Na^+/H^+ antiport activation in cultured rat aortic smooth muscle on calmodulin, calcium, and ATP. Evidence for the involvement of calmodulin-dependent kinases. *J Biol Chem* 263, 16780-16786.

Nakamura, TY, Iwata, Y, Arai, Y, Komamura, K, and Wakabayashi, S (2008). Activation of Na^+/H^+ exchanger 1 is sufficient to generate Ca^{2+} signals that induce cardiac hypertrophy and heart failure. *Circ Res* 103, 891-899.

Nakano, H, and Omura, S (2009). Chemical biology of natural indolocarbazole products: 30 years since the discovery of staurosporine. *J Antibiot (Tokyo)* 62, 17-26.

Ohmori, S, Sakai, N, Shirai, Y, Yamamoto, H, Miyamoto, E, Shimizu, N, and Saito, N (2000). Importance of protein kinase C targeting for the phosphorylation of its substrate, myristoylated alanine-rich C-kinase substrate. *J Biol Chem* 275, 26449-26457.

Orlowski, J, and Grinstein, S (2004). Diversity of the mammalian sodium/proton exchanger SLC9 gene family. *Pflugers Arch* 447, 549-565.

Pouyssegur, J, Sardet, C, Franchi, A, L'Allemain, G, and Paris, S (1984). A specific mutation abolishing Na^+/H^+ antiport activity in hamster fibroblasts precludes growth at neutral and acidic pH. *Proc Natl Acad Sci U S A* 81, 4833-4837.

MOL #89268

Sanchez, C, Mendez, C, and Salas, JA (2006). Indolocarbazole natural products: occurrence, biosynthesis, and biological activity. *Nat Prod Rep* 23, 1007-1045.

Sardet, C, Fafournoux, P, and Pouyssegur, J (1991). Alpha-thrombin, epidermal growth factor, and okadaic acid activate the Na^+/H^+ exchanger, NHE-1, by phosphorylating a set of common sites. *J Biol Chem* 266, 19166-19171.

Shimada-Shimizu, N, Hisamitsu, T, Nakamura, TY, and Wakabayashi, S (2013). Evidence that Na^+/H^+ exchanger 1 is an ATP-binding protein. *FEBS J* 280, 1430-1442.

Taylor, CW (2002). Controlling calcium entry. *Cell* 111, 767-769.

Toledo, LM, and Lydon, NB (1997). Structures of staurosporine bound to CDK2 and cAPK--new tools for structure-based design of protein kinase inhibitors. *Structure* 5, 1551-1556.

Toullec, D, Pianetti, P, Coste, H, Bellevergue, P, Grand-Perret, T, Ajakane, M, Baudet, V, Boissin, P, Boursier, E, Loriolle, F, et al. (1991). The bisindolylmaleimide GF 109203X is a potent and selective inhibitor of protein kinase C. *J Biol Chem* 266, 15771-15781.

Wakabayashi, S, Bertrand, B, Ikeda, T, Pouyssegur, J, and Shigekawa, M (1994a). Mutation of calmodulin-binding site renders the Na^+/H^+ exchanger (NHE1) highly H^+ -sensitive and Ca^{2+} regulation-defective. *J Biol Chem* 269, 13710-13715.

Wakabayashi, S, Bertrand, B, Shigekawa, M, Fafournoux, P, and Pouyssegur, J (1994b). Growth factor activation and " H^+ -sensing" of the Na^+/H^+ exchanger isoform 1 (NHE1).

MOL #89268

Evidence for an additional mechanism not requiring direct phosphorylation. *J Biol Chem* 269, 5583-5588.

Wakabayashi, S, Hisamitsu, T, and Nakamura, TY (2013). Regulation of the cardiac Na⁺/H⁺ exchanger in health and disease. *J Mol Cell Cardiol* 61, 68-76.

Wakabayashi, S, Nakamura, TY, Kobayashi, S, and Hisamitsu, T (2010). Novel phorbol ester-binding motif mediates hormonal activation of Na⁺/H⁺ exchanger. *J Biol Chem* 285, 26652-26661.

Wakabayashi, S, Pang, T, Su, X, and Shigekawa, M (2000). A novel topology model of the human Na⁺/H⁺ exchanger isoform 1. *J Biol Chem* 275, 7942-7949.

Wakabayashi, S, Shigekawa, M, and Pouyssegur, J (1997). Molecular physiology of vertebrate Na⁺/H⁺ exchangers. *Physiol Rev* 77, 51-74.

Walker, EH, Pacold, ME, Perisic, O, Stephens, L, Hawkins, PT, Wymann, MP, and Williams, RL (2000). Structural determinants of phosphoinositide 3-kinase inhibition by wortmannin, LY294002, quercetin, myricetin, and staurosporine. *Mol Cell* 6, 909-919.

MOL #89268

FOOTNOTE

This work was supported by Grants-in-Aid for Scientific Research (B) [Grant 23290046] and Exploratory Research [Grant 22659046] from the Ministry of Education, Culture, Sports, Science and Technology; and Intramural Research Fund [Grant 22-2-1] for Cardiovascular Diseases of the National Cerebral and Cardiovascular Center.

MOL #89268

Figure Legends

Fig. 1. Effects of various chemical compounds on the resting pH_i . (A) Changes in pH_i were measured using the pH indicator dye BCECF-AM. PS120 cells stably transfected with the wild-type NHE1 were stimulated with PMA (1 μM) in the absence or presence of 1 μM of the indicated compounds. St, staurosporine; drug 1, N,2-diphenyl-4-propylimidazo[1,2a]benzimidazole-1-carbothioamide; BIS1, bisindolylmaleimide I; K252a and K252c, staurosporine derivatives that possess an indolocarbazole ring. (B) Effects of EIPA (50 μM) and staurosporine (St) (1 or 10 μM) on the basal pH_i . Data are presented as means ($n > 20$ cells).

Fig. 2. Effects of various bisindolylmaleimide and indolocarbazole derivatives on PMA-induced cytoplasmic alkalinization. (A) Changes in pH_i were measured using the [^{14}C]benzoic acid equilibration method at 15 min after stimulation. NHE1 transfectants were stimulated with 1 μM PMA or 1 μM of each chemical. (B) Effects on PMA-induced cytoplasmic alkalinization. NHE1 transfectants were stimulated for 15 min with 1 μM PMA in the absence or presence of 1 μM of each chemical. The arrows represent significant inhibition ($p < 0.05$) (solid arrows, $>80\%$ inhibition; dotted arrows, $40\text{--}80\%$ inhibition). PMA-induced cytoplasmic alkalinization without drugs was in the range between $0.17\text{--}0.23$ pH units for different 24-well plates. Data are presented as means \pm standard deviation ($n = 3$),

MOL #89268

normalized to the values of PMA alone, which were set to 1.

Fig. 3. Effects of various bisindolylmaleimide and indolocarbazole derivatives on phenylephrine-induced cytoplasmic alkalinization. NHE1 transfectants were further stably transfected with α 1-adrenergic receptor (α 1-AR). Cells were stimulated for 15 min with α 1-AR agonist phenylephrine (Phe, 10 μ M) in the absence or presence of 1 μ M of each chemical. The leftmost column shows data for NHE1 transfectants without α 1-AR expression. Phenylephrine-induced cytoplasmic alkalinization without drugs was in the range between 0.15-0.20 pH units for different 24-well plates. Data are presented as means \pm standard deviation (n = 3), normalized to the values of phenylephrine alone, which were set to 1. * $P < 0.05$ versus phenylephrine alone.

Fig. 4. Effects of various bisindolylmaleimide and indolocarbazole derivatives on the activity of intracellular PKC. (A) Representative photographs showing the subcellular localization of GFP-tagged MARCKS protein. MARCKS-GFP is initially localized at the plasma membrane and dissociated from the plasma membrane via phosphorylation by PKC upon stimulation with PMA (1 μ M) (leftmost panels). The effect of PMA on the subcellular localization of MARCKS-GFP was examined in the presence of each indicated drug. St, staurosporine. (B) Summary of MARCKS-GFP dissociation from the plasma membrane. The dissociation index

MOL #89268

was calculated as described in the Experimental section. Data are presented as means \pm standard deviation ($n = 5$). The red dotted line indicates the dissociation index value corresponding to no change in the plasma membrane localization of MARCKS-GFP upon PMA stimulation. $*P < 0.05$ versus PMA alone.

Fig. 5. Fluorescence analysis of the LID peptide association with TNP-ATP. (A) Emission spectra of TNP-ATP in the absence or presence of the indicated peptides. Spectra were measured in the presence of 30 μ M TNP-ATP with or without 14 μ M of each peptide, at an excitation wavelength of 380 nm. GP57 corresponds to the NHE1 LID, the IL54 control peptide corresponds to the middle region of NHE1, and the mutant peptide LI-2A corresponds to GP57 with Leu-573 and Ile-574 replaced by two alanine residues. (B) Direct titration of TNP-ATP fluorescence with GP57 alone (control) or in addition to 5 mM non-fluorescent ATP or 100 μ M PtdIns(4,5) P_2 . The K_d values (mean \pm standard error) for GP57 binding to TNP-ATP, non-fluorescent ATP, and PtdIns(4,5) P_2 were determined to be 28.0 ± 1.8 μ M, 430 ± 42.7 μ M, and 22.3 ± 6.9 μ M, respectively.

Fig. 6. Effects of various chemical compounds on TNP-ATP fluorescence. (A) Typical traces for time course analysis of the GP57-induced increase in TNP-ATP fluorescence. In the upper left trace, GP57 (14 μ M) was added to a TNP-ATP solution (20 μ M), while in the other traces,

MOL #89268

initially 10 μM of each chemical was added (dotted arrows) followed by the addition of GP57 (solid arrows). (B) Summary of drug effects on the GP57-induced increase in fluorescence (ΔF). Each compound (10 μM) was first added to a TNP-ATP solution (20 μM) and then the fluorescence change induced by GP57 (14 μM) was monitored. For several chemicals (Go6976, KT5720, SB218078, rebeccamycin, and lestaurtinib), data were not obtained due to the disturbance caused by the strong fluorescence of these chemicals. Data are presented as means \pm SD ($n = 3$). * $P < 0.05$ versus no drug. n.d., no data.

Fig. 7. Concentration-dependent effects of three indolocarbazole compounds on TNP-ATP and PMA-induced cytoplasmic alkalinization. (A) Titration of TNP-ATP fluorescence with GP57 in the absence or presence of 10 μM staurosporine, UCN-01, or K252a. For curve fitting, we assumed that the maximal fluorescence intensity ($\Delta\text{F}_{\text{max}}$) was the same in the absence or presence of chemicals. The K_d values (mean \pm SE) for staurosporine, UCN-01, and K252a were determined to be 1.70 ± 0.05 μM , 2.54 ± 0.13 μM , and 3.35 ± 0.08 μM , respectively. (B–D) Concentration-dependent effects of staurosporine, UCN-01, and K252a on PMA-induced cytoplasmic alkalinization. The inhibition of alkalinization occurred in a concentration range (1–10 μM) that was similar to the K_d values. Data are presented as means \pm SD ($n = 3$).

MOL #89268

Fig. 8. Effects of staurosporine and the LID mutation on NHE1 activation induced by okadaic acid or hyperosmotic medium. (A) Changes in pH_i were measured using the [^{14}C]benzoic acid equilibration method at 15 min after stimulation. NHE1 transfectants were stimulated with 1 μM of the indicated phosphatase inhibitors. The inhibition of okadaic acid (OA)-induced cytoplasmic alkalinization by 1 μM staurosporine (St) was also assessed. Data are presented as means \pm standard deviation ($n = 3$). (B) Effect of different concentrations of staurosporine on cytoplasmic alkalinization in NHE1 transfectants in response to hyperosmotic medium (HBS + 100 mM sucrose). (C and D) Effects of OA and hyperosmolarity on the subcellular localization of MARCKS-GFP. Unlike PMA, these stimuli did not induce the dissociation of MARCKS-GFP from the plasma membrane. (E) Changes in pH_i were measured using the [^{14}C]benzoic acid equilibration method 15 min after stimulation. Cells expressing wild-type or mutant NHE1 (LI-2A) were stimulated with 1 μM PMA, 10 μM phenylephrine, 1 μM okadaic acid, or 100 mM sucrose. In the experiment with phenylephrine, cells stably expressing the α_1 -adrenergic receptor and NHE1 were used. In one experiment, cells were pre-treated for 30 min with 5 mM 2-deoxyglucose (for ATP depletion). Data are presented as means \pm standard deviation ($n = 3$).

Fig. 9. Effect of staurosporine on the plasma membrane translocation of GFP-labeled LID in response to various stimuli. Stable NHE1 transfectants were further transfected with GFP-LID.

MOL #89268

In (C), the NHE1/ α 1-adrenergic receptor transfectants were transfected with GFP-LID. (A) Cells were incubated 15 min without additional chemicals. (B–E) Plasma membrane translocation of GFP-LID after the addition of 1 μ M PMA, 10 μ M phenylephrine (Phe), 1 μ M okadaic acid or 100 mM sucrose (hyper), and inhibition of translocation by staurosporine (St, 1 μ M), but not BIS1 (1 μ M). (F) Inhibition of membrane translocation in cells treated for 15 min with the metabolic inhibitor 2-deoxyglucose (5 mM) to deplete the cellular ATP prior to the addition of 1 μ M of PMA. (G) GFP-LID localization in cells stimulated for 15 min with 1 μ M PMA (left panel), and then treated with 5 mM 2-deoxyglucose (2-DOG) (right panels). (Inset) Line profile analysis.

Fig. 10. Schematic model of NHE1 regulation via the LID. In the resting state, NHE1 maintains basal activity via interaction with ATP or acidic phospholipids. Upon stimulation of the Gq-coupled receptor, diacylglycerol (DAG)/phorbol esters (PEs) interact with the LID, inducing a conformational change of the LID and an increase in the affinity of the LID for acidic phospholipids, which in turn results in an increase in H⁺ affinity for NHE1. Okadaic acid or hyperosmolarity may also activate NHE1, possibly via LID. Treatment with indolocarbazole compounds attenuates the interaction of ATP or acidic phospholipids with LID, and thereby inhibits NHE1 activity. ATP depletion would promote ATP dissociation from NHE1 and reduce the membrane level of acidic phospholipids via inhibition of lipid kinases.

MOL #89268

Consequently, ATP depletion would facilitate the separation of LID from the plasma membrane and result in a drastic inhibition of exchange activity. Notably, under the coexistence of an activator and an inhibitor, the NHE1 conformation would be balanced between the most activated and the most inhibited states, according to their relative amounts interacting to the LID,.

Figure 1

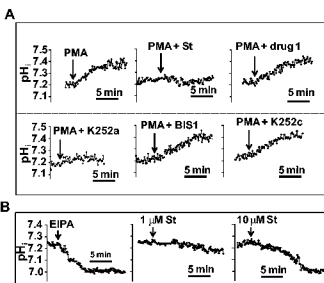


Figure 2

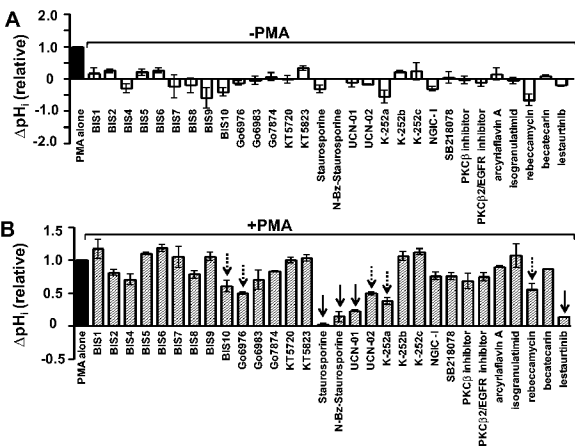


Figure 3

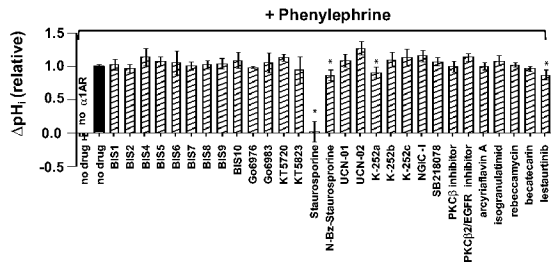


Figure 4

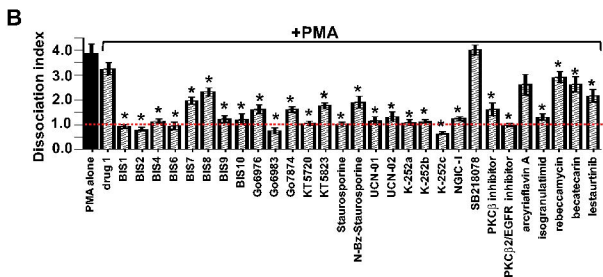
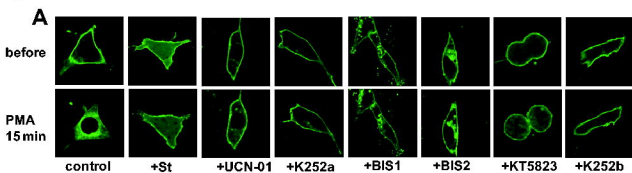


Figure 5

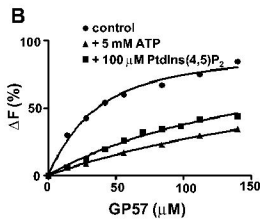
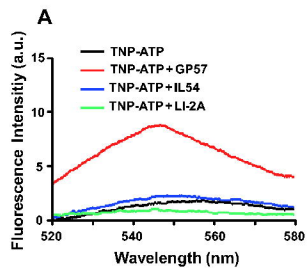


Figure 6

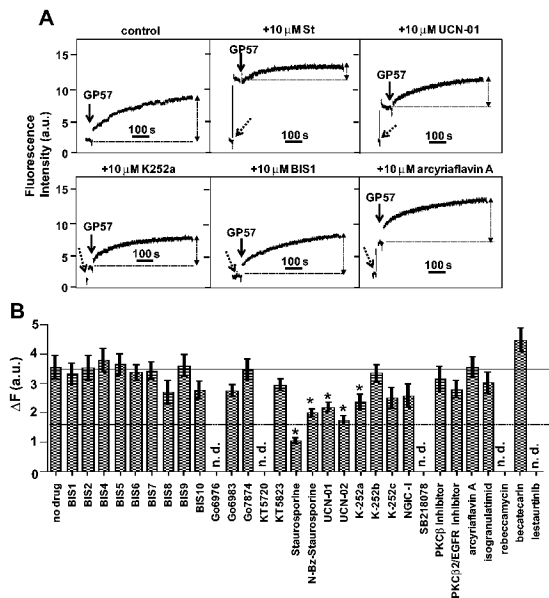


Figure 7

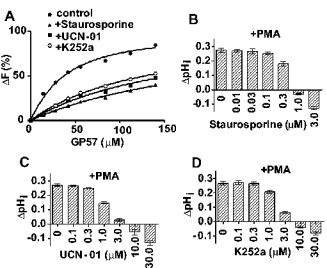


Figure 8

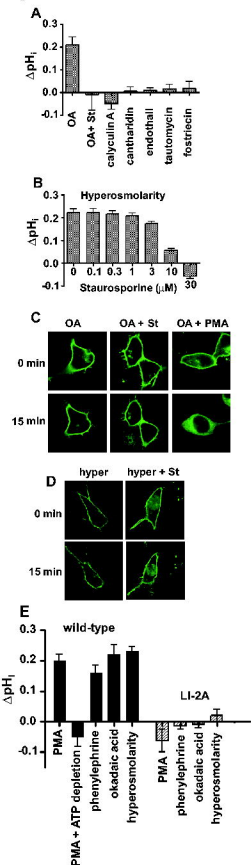


Figure 9

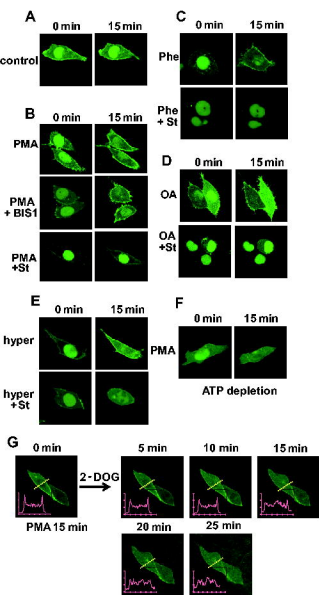


Figure 10

